THE JOURNAL OF BIOLOGICAL CHEMISTRY VOL. 285, NO. 1, pp. 357–364, January 1, 2010

Bordetella Adenylate Cyclase Toxin Promotes Calcium Entry into Both CD11b$^+$ and CD11b$^-$ Cells through cAMP-dependent L-type-like Calcium Channels*[S]

Received for publication, April 3, 2009, and in revised form, October 27, 2009 Published, JBC Papers in Press, October 29, 2009, DOI 10.1074/jbc.M109.003491

César Martín, Geraxane Gómez-Bilbao[1], and Helena Ostolaza[2]

From the Unidad de Biofísica (Centro Mixto CSIC-UPV/EHU) and Departamento de Bioquímica, Universidad del País Vasco, Aptdo. 644, 48080 Bilbao, Spain

Adenylate cyclase toxin (ACT), a 200 kDa protein, is an essential virulence factor for *Bordetella pertussis,* the bacterium that causes whooping cough. ACT is a member of the pore-forming RTX (repeats-in-toxin) family of proteins that share a characteristic calcium-binding motif of Gly- and Asp-rich nonapeptide repeats and a marked cytolytic or cytotoxic activity. In addition, ACT exhibits a distinctive feature: it has an N-terminal calmodulin-dependent adenylate cyclase domain. Translocation of this domain into the host cytoplasm results in uncontrolled production of cAMP, and it has classically been assumed that this surge in cAMP is the basis for the toxin-mediated killing. Several members of the RTX family of toxins, including ACT, have been shown to induce intracellular calcium increases, through different mechanisms. We show here that ACT stimulates a raft-mediated calcium influx, through its cAMP production activity, that activates PKA, which in turn activates calcium channels with L-type properties. This process is shown to occur both in CD11b$^+$ and CD11b$^-$ cells, suggesting a common mechanism, independent of the toxin receptor. We also show that this ACT-induced calcium influx does not correlate with the toxin-induced cytotoxicity.

Adenylate cyclase toxin (ACT)[3] is a crucial virulence factor secreted by *Bordetella pertussis*, the bacterium that causes whooping cough (1). ACT is a single polypeptide chain of 1706 amino acid residues that consists of an adenylate cyclase domain corresponding to the 400 N-terminal residues (AC domain) and a characteristic RTX (Repeats in Toxin) hemolysin domain comprising the C-terminal 1306 residues (2). The hemolysin domain consists in turn of a hydrophobic (channel-forming) domain (residues 500–700), an acylation domain (residues 800–1000), and a characteristic glycine/aspartate-rich repeats domain (residues 1000–1600), typically present in the members of the RTX family of proteins to which ACT belongs (3, 4). Binding of calcium to these repeats induces conformational changes in the toxin molecule (5, 6) necessary for the toxin functionality. The RTX moiety insertion into cellular membranes is necessary to mediate the translocation of the AC catalytic domain into the cytosol of host cells, myeloid phagocytes that express the integrin receptor CD11b/CD18, and upon activation by cellular calmodulin, it catalyzes an uncontrolled conversion of ATP into cAMP, a process often referred to as "intoxication" (7, 8). The RTX domain accounts as well for the hemolytic activity of ACT (9–11). This toxin can form cation-selective pores in cell membranes independent of translocation, thereby perturbing ion homeostasis. This pore-forming activity has been reported to contribute to the cytotoxic action of ACT by cooperating with cAMP in promoting cell death (12, 13). More recently, Fiser *et al.* (14) have reported a third activity of ACT, which involves a sustained rise of $[Ca^{2+}]_i$ promoted by membrane translocation of the AC domain (14).

Several members of the RTX family of toxins have been shown to induce intracellular calcium rises, through different mechanisms. Earlier studies carried out with LktA, the leukotoxin secreted by *Pasteurella hemolytica,* demonstrated that its interaction with bovine leukocytes induced intracellular calcium increase by influx of extracellular Ca^{2+} through voltage-gated channels (15–17). Similar findings were reported in human neutrophils and human natural killer cells by leukotoxin (LTx) from *Actinobacillus actinomycetemcomitans* (18, 19). In the case of LktA, using alveolar macrophages, cation entry was shown to be inhibited by pertussis toxin, inhibitors of phospholipases A_2 and C and the arachidonic acid analog 5,8,11,14-eicosatetraynoic acid, suggesting that the LktA-induced $[Ca^{2+}]$ increase involves a G protein-coupled activation of L-type Ca^{2+} channels (20), while in the case of LTx a mobilization of store-operated channels has been involved in the toxin-induced calcium rise (21). For *Escherichia coli* α-hemolysin (HlyA) a controversy exists about the mechanism by which it promotes calcium influx into cells. Whereas Uhlen *et al.* (2000) reported that sublytic concentrations of HlyA stimulate oscillatory calcium responses through activation of L-type calcium channels

* This work was supported by grants from the Spanish Ministerio de Ciencia y Tecnología (Project BFU 2007–62062), the Basque Government (ETORTEK Program), and the University of Basque Country (UPV/EHU, Project UE06/10).

[S] The on-line version of this article (available at http://www.jbc.org) contains supplemental Figs. S1–S4.

[1] Recipient of a predoctoral fellowship from the University of Basque Country.

[2] To whom correspondence should be addressed. Fax: 34-94-601.33.60; E-mail: gbzoseth@lg.ehu.es.

[3] The abbreviations used are: ACT, adenylate cyclase toxin; PKA, cAMP-dependent protein kinase; MβCD, methyl-β-cyclodextrin; CHO, Chinese hamster ovary cells; LDH, lactate dehydrogenase; RLMD, raft-like membrane domain; $[Ca^{2+}]_i$, free cytosolic calcium concentration; AC domain, N-terminal enzymatic adenylate cyclase domain; db-cAMP, N^6,2′-*O*-dibutyryladenosine 3′,5′-cyclic monophosphate; 8-Br-cAMP, 8-Br-adenosine-3′,5′-cyclic monophosphate; CaM, calmodulin; NEBD, nuclear envelope breakdown; VOC, voltage-operated channels; TIRFM, total internal reflection fluorescence microscopy; PLD1, phospholipase D1; ARNO, member of the family of guanine nucleotide exchange factors for ARFs; ARF, ADP-ribosylation factor; DMEM, Dulbecco's modified Eagle's medium.

(22), other authors reported that this toxin promotes rises of $[Ca^{2+}]_i$ by allowing passive influx of calcium ions through the toxin pores (23, 24). In the case of ACT, it has been proposed that the mechanism by which this toxin induces $[Ca^{2+}]_i$ rises in macrophages appears to be independent of both adenylate cyclase activity and the pore-forming activity of the toxin, but dependent on interaction of the toxin with its receptor, the integrin CD11b/CD18, and on the translocation of the catalytic domain that appears to participate itself in the formation of a novel type of membrane path for calcium ions (14). ACT has also been reported to rise $[Ca^{2+}]_i$ in non-immune cells, such as pancreatic beta-cells and myocytes that do not contain the integrin receptor through L-type calcium channels (25, 26).

Perturbation of cellular calcium homeostasis seems indeed to be a common feature in many strategies followed by pathogens to damage host cells and cause diseases (27). Most cells, including hematopoietic cells, contain specialized signaling microdomains that support the generation of highly localized Ca^{2+} signals (28, 29). This phenomenon has been referred to as "geography of Ca^{2+} signals" to draw attention to the fact that this signaling system has a precise spatial and temporal organization (30). In connection with this phenomenon, raft-like membrane microdomains and caveolae exist in most cells as organized structures involved in the regulation of both Ca^{2+} entry into cells and Ca^{2+}-dependent signal transduction (31), besides concentrating other molecular machineries responsible for a variety of different signaling pathways (32).

We show here that ACT induces a receptor-independent, microdomain-related calcium influx through activation of non-voltage-dependent calcium channels with L-type properties upon activation of PKA via the toxin-induced cAMP production. Our results extend and somehow correct previous work from Fiser *et al.* (14). We also show that this ACT-induced calcium influx does not correlate with the toxin-induced cytotoxicity.

EXPERIMENTAL PROCEDURES

Reagents—$LaCl_3$, (±) Bay K 8644, methyl-β-cyclodextrin, nifedipine, diltiazem, verapamil, 2-aminoethyl diphenilborinate (2-APB), gramicidin A, U73122, and pertussis toxin (PTx) were from Sigma; KT5720 and AACOCF3 were from Calbiochem (Merck, Germany); Fura2-AM, Oligofectamine™ transfection reagent and bis-oxonol were from Invitrogen. Antibodies to L-type Ca^{2+} α1C and siRNA against L-type Ca^{2+} α1C and control siRNA were purchased from Santa Cruz Biotechnologies.

ACT and proACT Purification—ACT and proACT were expressed in *E. coli* XL-1 blue cells (Stratagene) transformed with pT7CACT or pACT7 plasmids, and purified as previously described (33). In this protocol, urea is used, and final purified protein samples contain urea. The corresponding urea controls were carefully done, and no effect was found regarding the induction of a calcium influx.

Cell Culture—J774A.1 murine macrophages (ATTC number TIB-67) and CHO cells (ATTC number CCL-61) were cultured at 37 °C in DMEM supplemented with 10% (v/v) heat-inactivated fetal bovine serum, 100 units/ml penicillin, 100 μg/ml streptomycin, and 4 mM L-glutamine in 5% CO_2.

Measurements of Intracellular $[Ca^{2+}]$—J774A.1 and CHO cells grown on glass coverslips were loaded with 2 μM Fura2-AM for 30–45 min in DMEM at 37 °C, and washed in 20 mM Tris-HCl, 2.4 mM $CaCl_2$, 10 mM glucose, pH 7.4. The coverslips were mounted on a thermostatized perfusion chamber on a Nikon Eclipse TE 300-based microspectofluorometer and visualized with a ×40 oil-immersion fluorescence objective lens. At the indicated time, 35 nM ACT was added, and the intracellular Ca^{2+} levels were determined using the method of Grynkiewicz *et al.* (34). The 340/380 nm excited light ratio was determined with a Delta-Ram system (Photon Technologies International, Princeton) and converted into Ca^{2+} concentration from the standard equation: $[Ca^{2+}]_i = K_D \times Q \times (R - R_{min})/(R_{max} - R)$, where K_D is the Ca^{2+} dissociation constant of Fura2. R represents the ratio of the fluorescence intensities measured at 340 and 380 nm; R_{max} and R_{min} were found when Fura2 was saturated with Ca^{2+} and when completely free of Ca^{2+}, respectively. Q is the ratio of the minimum/maximum fluorescence intensity at 380 nm, *i.e.* the fluorescence intensity measured when Fura2 is free of Ca^{2+} and saturated with Ca^{2+}, respectively.

Erythrocytes, at ~1% hematocrit, and neutrophils were loaded with 2 μM Fura2-AM for 45 min at 37 °C, washed, and resuspended in 20 mM Tris-HCl, 0.25 M glucose, and 2.4 mM $CaCl_2$, pH 7.4 at 0.1% hematocrit and 0.5×10^6 cell/ml, respectively. Cells were transferred into a quartz cuvette for fluorescence measurements in a Varian Cary Eclipse fluorometer, and the intracellular Ca^{2+} levels were determined as described above.

Transfection of J774A.1 Cells with siRNA—50% confluent cells were transfected with 20 nM siRNA against L-type Ca^{2+} α1C using oligofectamine™ transfection reagent in OPTIMEM medium (Invitrogen) as directed by the manufacturer. 5 h following transfection medium was supplemented with fetal bovine serum, and the incubation continued for 72 h. A scrambled sequence siRNA was used as a negative control.

Western Analysis—To verify L-type Ca^{2+} α1C silencing, total cell proteins of control and silenced cells were analyzed by Western blot. Proteins were separated electrophoretically on a 10% SDS-polyacrylamide gel and transferred to nitrocellulose membrane. The membranes were then blocked overnight at 4 °C, and after 2 h of incubation with the primary antibody, membranes were washed and exposed to the secondary antibody for 1 h at room temperature. Proteins were detected using the enhanced chemiluminiscence detection system (ECL®, Amersham Biosciences). The Quantity One® Image Analyzer software program (Bio-Rad) was used for quantitative densitometric analysis.

RNA Isolation and RT-PCR—RNA isolation and RT-PCR were performed using TRIzol® reagent (Invitrogen) and OneStep RT-PCR kit (Qiagen), respectively. The primers used to amplify α1C and β-subunits transcripts have been described previously (35, 36).

Confocal Microscopy—Control and transfected cells grown onto 12-mm diameter glass coverslips were fixed for 10 min with 3.7% paraformaldehyde and permeabilized with acetone at −20 °C. Then samples were incubated with the anti-L-type Ca^{2+} α1C primary antibody for 1 h followed by incubation with

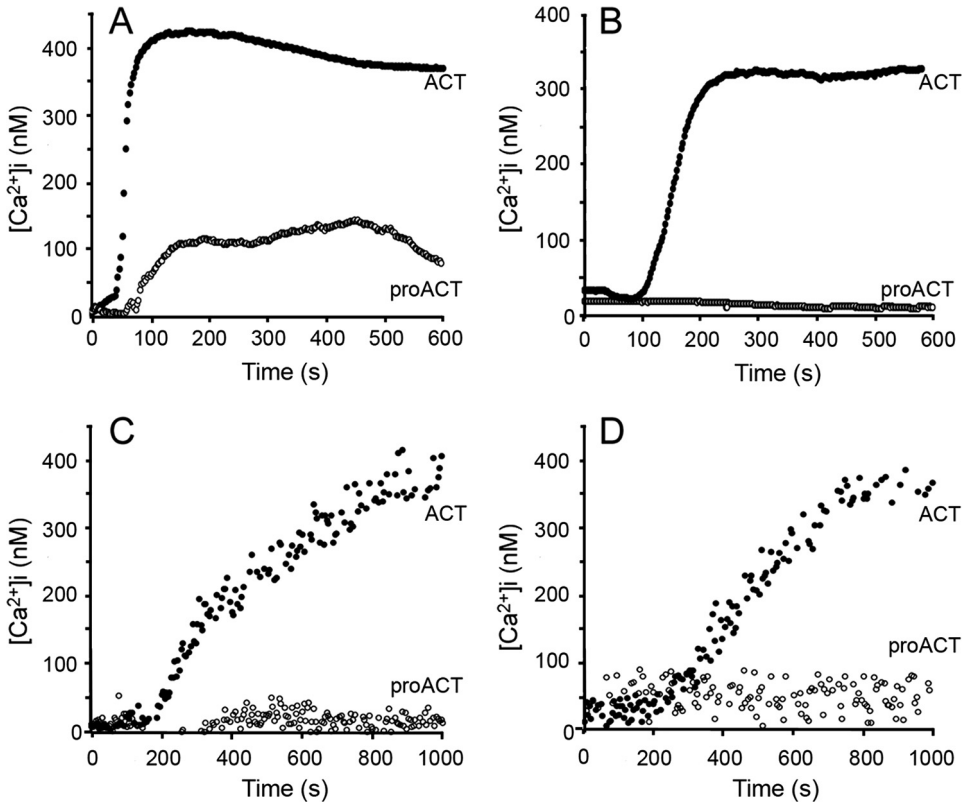

FIGURE 1. **Kinetics of ACT-induced intracellular calcium increase in J774A.1 macrophages (*A*), CHO cells (*B*), human neutrophils (*C*), and human erythrocytes (*D*) incubated with 35 nM acylated ACT (●) or with the same concentration of the non-acylated toxin form, pro-ACT (○).** Toxin was added after 60 s.

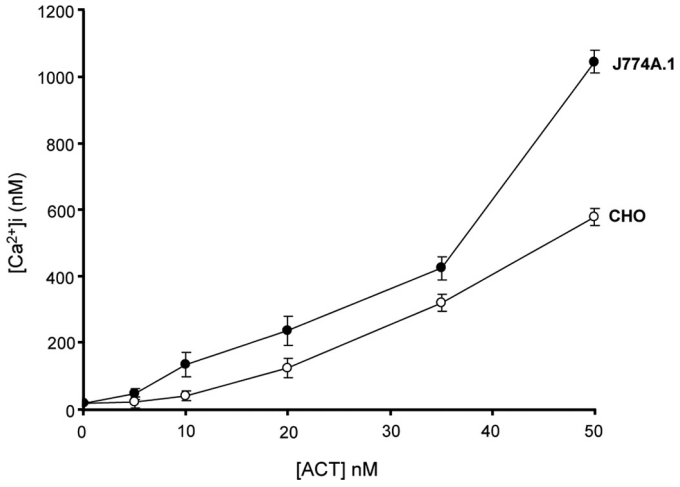

FIGURE 2. **ACT concentration dependence on the toxin-induced intracellular calcium rise in J774A.1 and CHO cells.**

fluorescein isothiocyanate-conjugated secondary antibody. Coverslips were mounted on a glass slide, and samples were visualized using a confocal microscope (Olympus IX 81) with sequential excitation and capture image acquisition with a digital camera (Axiocam NRc5, Zeiss). Images were processed with Fluoview v.50 software.

Determination of cAMP—A total of 10^6 J774A.1 cells were incubated with 35 nM or 100 nM ACT for 30 min in DMEM without fetal calf serum. The reaction was stopped by addition of ice-cold acidified ethanol. The samples were centrifuged, and the concentration of cAMP in the supernatants was determined by a competition immunoassay as described by the manufacturer (GE Healthcare).

Cytotoxicity Assay—ACT-induced cytotoxicity was determined through release of lactate dehydrogenase (LDH) into the culture medium by the method of Bergmeyer and Bernt (37). Cytotoxicity is expressed as percent LDH released into the medium relative to the total LDH content.

Statistical Analysis—All measurements were performed at least three times, and results are presented as mean ± S.D. Levels of significance were determined by a two-tailed Student's *t* test, and a confidence level of greater than 95% ($p < 0.05$) was used to establish statistical significance.

RESULTS

ACT Promotes a Rapid Intracellular Calcium Rise Both in $CD11b^+$ and $CD11b^-$ Cells—The natural targets for ACT are reported to be myeloid phagocytic cells such as macrophages, neutrophils, and dendritic cells, which express the integrin receptor $\alpha_M\beta_2$ (CD11b/CD18, CR3, or Mac-1) to which the toxin binds with high affinity (38). However, the toxin has been shown to bind and intoxicate, with variable efficiency, a large variety of cell types lacking this receptor, such as myocytes, pancreatic beta-cells, fibroblasts, epithelial cells, T-lymphocytes, or mammalian erythrocytes, among others (39, 40, 9).

We show here that exposure of both $CD11b^+$ cells, *e.g.* J774A.1 cells, and $CD11b^-$ cells, *e.g.* CHO, to low doses of purified ACT caused a very significant rise in $[Ca^{2+}]_i$, as demonstrated by fluorescence microscopy measurements using the calcium-sensitive probe Fura-2 AM (Fig. 1). ACT induced in both cases a calcium elevation of similar amplitude and kinetics (Fig. 1, *A* and *B*). The ACT-induced calcium increase was concentration-dependent for all the cell types tested in the 5–50 nM toxin concentration range (Fig. 2). The ability of the toxin to mobilize $[Ca^{2+}]_i$ in both $CD11b/CD18^+$ and $CD11b/CD18^-$ cells indicates that interaction with the integrin receptor is not essential to induce this effect. As further shown in Fig. 1, the non-acylated form of the protein did not induce a comparable Ca^{2+} influx in none of the cell types tested, confirming that toxin palmitoylation is key to its functionality. Results obtained with human neutrophils ($CD11b/CD18^+$) and erythrocytes ($CD11b/CD18^-$) using fluorescence spectroscopy were qualitatively very similar (Fig. 1, *C* and *D*).

ACT-induced Calcium Influx Is Dependent on cAMP-dependent Activation of PKA—According to the findings of Fiser *et al.* (14), translocation of the toxin AC domain was essential for the toxin to induce a sustained calcium increase.

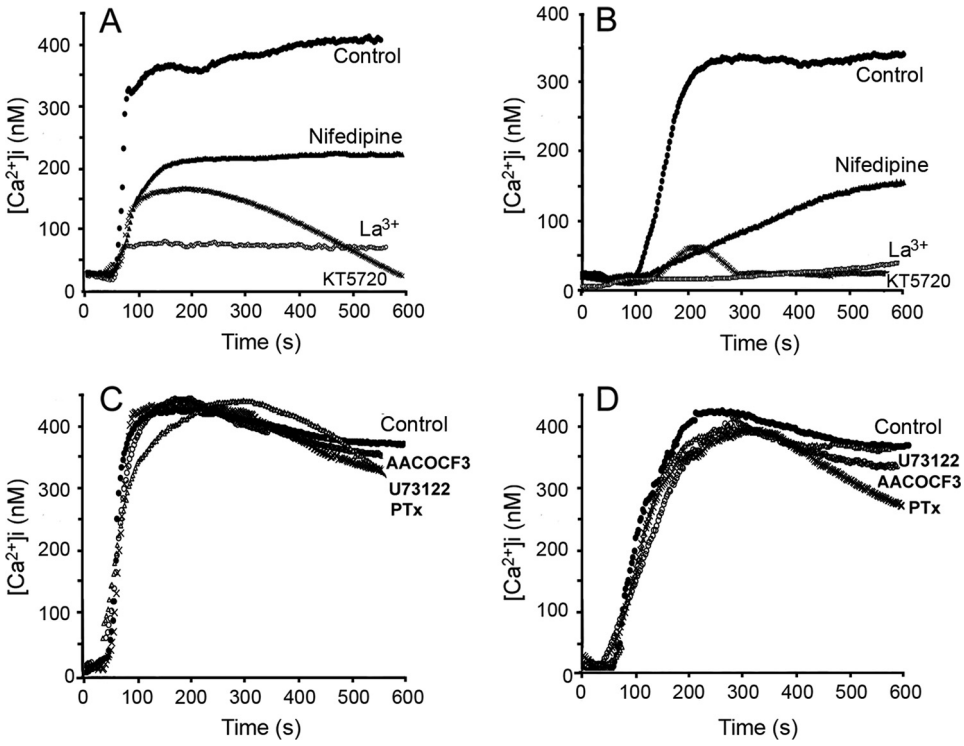

FIGURE 3. Kinetics of ACT-induced intracellular calcium increase in J774A.1 macrophages (*A*) and in CHO cells (*B*) incubated with 35 nM acylated ACT (●), or cells previously preincubated with various calcium channel inhibitors: 100 μM La^{3+}, 10 μM nifedipine, or 56 μM KT5720. Toxin was added after 60 s. Effect of 100 μM $AACOCF_3$ (○), 2 mM U73122 (△), or 2 ng/ml pertussis toxin (X) on the kinetics of ACT-induced intracellular calcium increase in J774A.1 macrophages (*C*) and in CHO cells (*D*) incubated with 35 nM acylated ACT (●).

The primary consequence of this catalytic domain translocation is the formation of high levels of cAMP, a second messenger broadly known to act through activation of protein kinase A. PKA, in turn, is known to phosphorylate, thus activating L-type calcium channels.

After incubation of the cells with 56 μM KT5720, a selective inhibitor of cAMP-dependent PKA, we found that the ACT-mediated $[Ca^{2+}]_i$ increase was almost completely suppressed, both in J774A.1 and in CHO cells (Fig. 3, *A* and *B*) supporting our hypothesis that L-type calcium channels might be mediating the toxin-induced calcium entry.

We found that ACT-mediated $[Ca^{2+}]_i$ rise was very significantly blocked upon preincubation of cells with 10 μM nifedipine, a prototypic antagonist of L-type calcium channels. The inhibitory effect of nifedipine was reproduced both in CD11b/CD18-positive (J774A.1 cells) and -negative cells (CHO cells) (Fig. 3, *A* and *B*). We extended these observations using representative drugs from two other L-type Ca^{2+} channel antagonists structurally unrelated to nifedipine: verapamil, which belongs to the phenylalkylamines category, and diltiazem, a component of the benzothiazepine family. As shown in supplemental Fig. S1*A*, both inhibitors blunted significantly the ACT-induced Ca^{2+} influx. The stimulation of a rapid calcium entry observed upon incubation of J774A.1 macrophages with (±) Bay K 8644, a prototypic agonist of L-type channels, and the inhibition of this calcium influx by the antagonists nifedipine and verapamil also correlates with the presence of L-type calcium channels in these cells (supplemental Fig. S1*B*).

An important point to evaluate was the possible contribution of a capacitative Ca^{2+} entry in the ACT-mediated calcium rise, as in a recent contribution (41) it has been argued that nifedipine, at high concentrations, has inhibitory effects on capacitative Ca^{2+} influx in Jurkat T cells. It can be seen in supplemental Fig. S2, that under conditions in which capacitative Ca^{2+} entry is completely inhibited with 2-APB, addition of ACT promoted a $[Ca^{2+}]_i$ rise with similar kinetics and amplitude than in the absence of inhibitor, and that cation entry was inhibited by nifedipine, supporting again the idea that ACT stimulates $[Ca^{2+}]_i$ rise via a mechanism that is independent of capacitative Ca^{2+} entry and dependent on L-type Ca^{2+} channels.

Effects of other known inhibitors of intracellular Ca^{2+} regulation routes were also tested. 100 μM AACOCF3, inhibitor of phospholipase A_2, U73122, inhibitor of phospholipase C, and pertussis toxin, that inhibits G_i proteins were used. Preincubation of cells with these compounds did not significantly affect the ACT-induced calcium influx (Fig. 3, *C* and *D*), suggesting that the corresponding routes are not involved in the toxin-mediated $[Ca^{2+}]_i$ rise.

Classical L-type calcium channels are voltage-gated and most typically express in excitable cells. Several reports have documented, however, the presence of non-voltage-dependent L-type calcium channels in various non-excitable cells such as T and B cells, or in mouse and human macrophages (36, 42, 43). Patch clamp experiments were performed in the J774A.1 macrophages used in this study, but no L-type calcium currents could be recorded (data not shown), suggesting that L-type like calcium channels in the J774A.1 macrophages do not respond to a voltage activation.

Using different approaches we detected, both by confocal microscopy, Western blot, and RT-PCR, expression of the L-type α1C subunit in the J774A.1 macrophages (Fig. 4, *A* and *B*). Transfection experiments with siRNA anti L-type α1C subunit and the proper siRNA controls were also done. siRNA anti-α1C down-regulated the surface expression of the α1C protein as shown by confocal microscopy (Fig. 4*A*). Western blot analysis confirmed this decrease in expression of the L-type α1c subunit only in anti-α1C siRNA-transfected cells (about 45 ± 5% decrease) but not in control siRNA cells (Fig. 4*B*). RT-PCR of mRNA from J774A.1 cells demonstrated that these cells express a transcript for the α1C subunit, and the auxiliary β-subunits, which play an important role in chaperoning α1C proteins to the cell surface, are also transcribed (Fig. 4*B*). Treatment of the α1c siRNA-transfected cells with the toxin showed

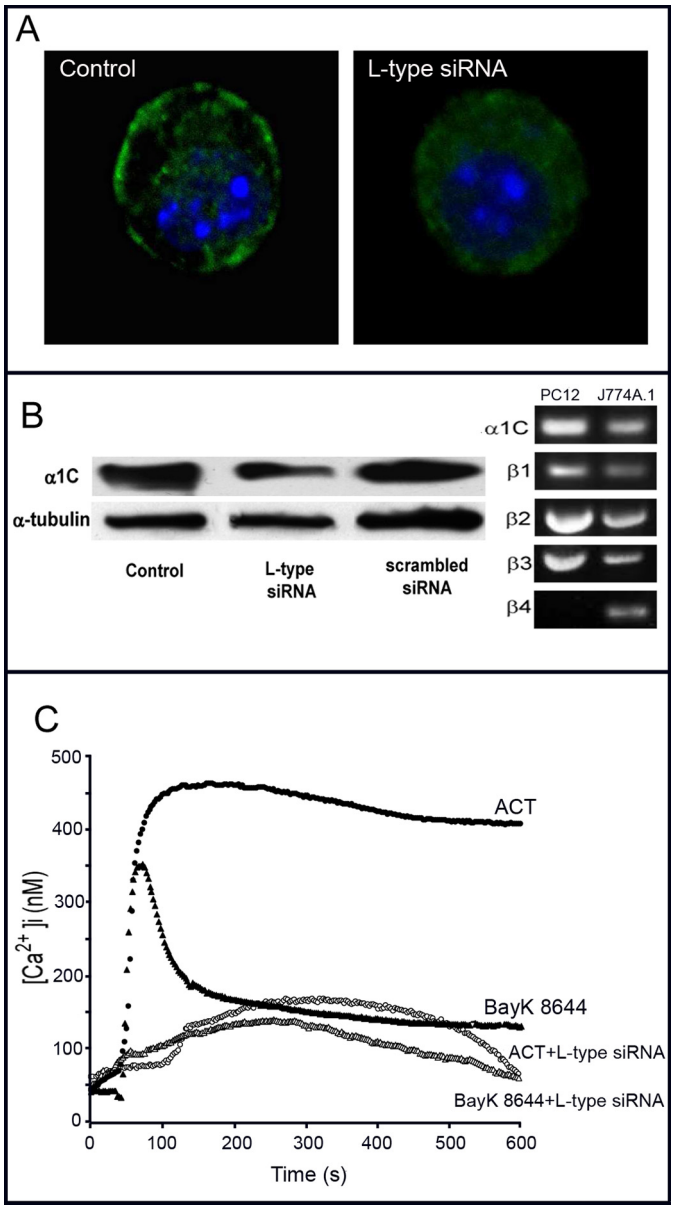

FIGURE 4. **Effect of transfecting J774A.1 cells with siRNA anti-L-type α1C subunit.** *A*, α1C expression in control and transfected cells analyzed by confocal microscopy. *B*, α1C expression in total cell lysate analyzed by Western blotting in control and transfected cells and control of transfection with a scrambled siRNA. The *lower panel* represents α-tubulin loading control (*left-hand side*). Detection of the mRNA of α1C and the four auxiliary β-subunits in J774A.1 macrophages. PC12 cells were used as control (*right-hand side*). *C*, kinetics of a toxin- and Bay K 8644-induced intracellular calcium rise in control and transfected cells. 35 nM ACT, control cells (●), 35 nM ACT, transfected cells (○), 100 nM Bay K8644, control cells (▲), and 100 nM Bay K8644, transfected cells (△).

now a very marked decrease in calcium rise. As might be expected, the effect of the agonist (±) Bay K 8644 was substantially reduced in anti-α1C siRNA-transfected cells (Fig. 4*C*).

We finally performed experiments in depolarized cells to test whether membrane depolarization is important in the toxin-induced calcium entry identified in this study. Our first observation was that ACT was able to induce an almost identical calcium rise both in polarized and in depolarized cells (supplemental Figs. S1*A* and S3*A*) The second observation was that the inhibitory effect of the three antagonists nifedipine, diltiazem, and verapamil on the ACT-induced calcium rise was also very similar in both polarized and depolarized cells (supplemental Figs. S1*A* and S3*A*). As a control, we confirmed with the fluorescent probe bis-oxonol that neither ACT nor its antagonists altered the plasma membrane potential and that with 50 mM KCl cells were completely depolarized (supplemental Fig. S3*B*). A third observation was that in the depolarized cells, the agonist Bay K 8644 was also able to induce a rapid calcium entry, similar to that observed in polarized cells, and that this influx was inhibited both by nifedipine and verapamil (supplemental Figs. S1*B* and S4*A*). We concluded from these results that non-voltage-dependent calcium channels with L-type properties are instrumental in the ACT-induced intracellular calcium rise.

Cholesterol Depletion and Low Temperature Impair ACT-induced Calcium Influx—Current evidence for the significant localization of ionic channels participating in calcium-induced signaling paths, including α1C subunits of L-type channels (36, 44), in raft-like membrane domains (RLMD) led us to hypothesize that ACT might induce a raft-mediated $[Ca^{2+}]_i$ increase. To test this hypothesis, we explored the effect of RLMD-perturbing agents and the effect of the temperature on the ACT-induced calcium influx. The latter parameter was investigated because calcium influx has been proposed to occur through translocation of the toxin AC domain (14), and translocation has been reported to be temperature-dependent (45).

Removing cholesterol from the membrane by preincubation of cells with methyl-β-cyclodextrin (MβCD), an agent known to disrupt RLMD (46), impaired the toxin ability to induce calcium influx (Fig. 5, *A–D*). The figure also shows that at 10 °C, calcium entry was completely abolished, probably because cAMP formation by the toxin AC domain translocation is very sensitive to temperature, becoming abrogated below ~20 °C (45). The high sensitivity of calcium entry to cholesterol depletion suggested that cation influx required the integrity of the RLMDs. Our finding that cAMP production by ACT was also affected by MβCD (Fig. 6) confirmed the latter requirement and suggested that the toxin must be RLMD-bound to cause cAMP production and calcium influx. The lack of effect of nifedipine or $LaCl_3$ on cAMP production (Fig. 6) indicated that translocation of the AC domain is independent of calcium influx.

ACT-induced Calcium Influx Does Not Correlate with Toxin-induced Cytotoxicity—An important question was whether the ability of the toxin to increase $[Ca^{2+}]_i$ contributed to its cytotoxicity. Blocking calcium entry by nifedipine or KT5720 did not prevent ACT killing of J774A.1 (Fig. 7). Also ACT-induced toxicity in CHO cells was much lower than in J774A.1 cells (Fig. 7), even if Ca^{2+} entry was about the same (Fig. 1). MβCD however affected very significantly toxin-induced cytotoxicity (Fig. 7). MβCD inhibits cAMP production by ACT (Fig. 6). Thus, calcium influx is not primarily responsible for the cytotoxic effect of ACT, but rather toxin-induced cytoxicity seems mainly caused by subversive effects of the second messenger cAMP in the cells.

DISCUSSION

ACT belongs to the so-called RTX family of bacterial protein toxins. Though it was initially believed that this family of toxins

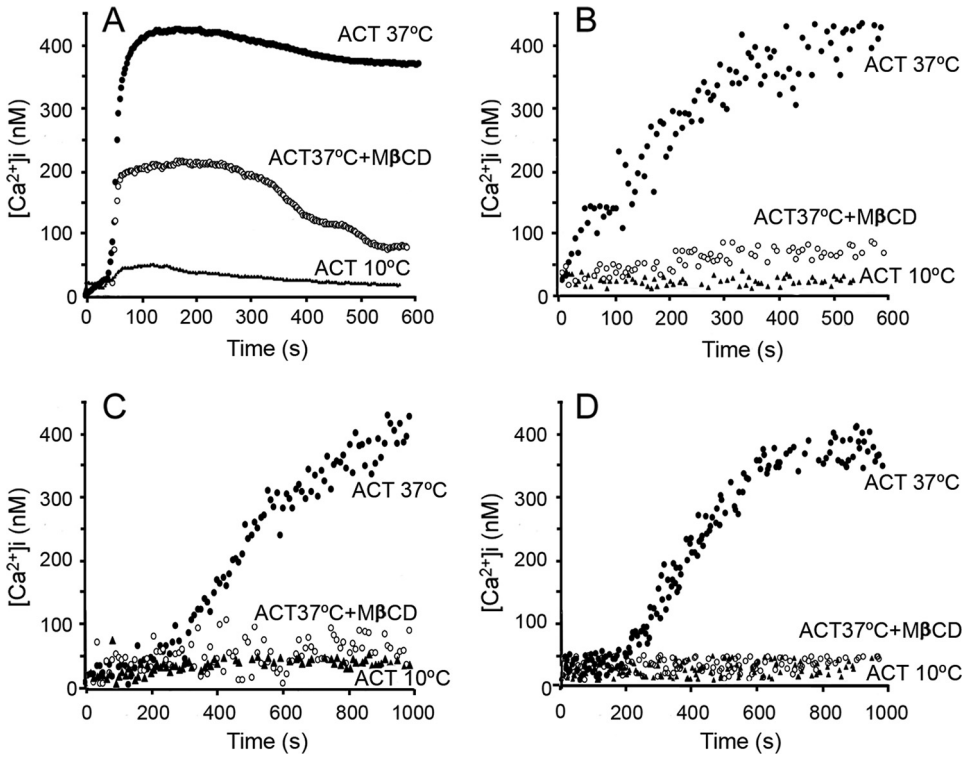

FIGURE 5. **Effect of temperature and cholesterol depletion on the kinetics of ACT-induced intracellular calcium increase in J774A.1 macrophages (*A*), CHO cells (*B*), human neutrophils (*C*), and human erythrocytes (*D*).** Cells were incubated with 35 nM acylated ACT at 37 °C (●) or 10 °C (▲) or previously preincubated with 10 mM MβCD for 30 min and then incubated with the toxin at 37 °C (○). Toxin was added after 60 s.

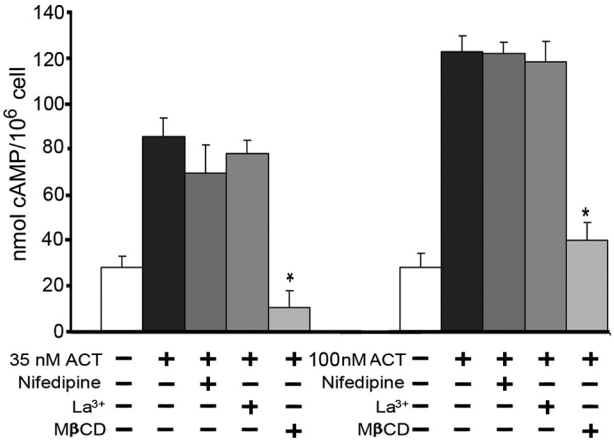

FIGURE 6. **Effect of calcium influx blocking and cholesterol depletion on the ACT production of cAMP.** The concentrations of nifedipine, La^{3+}, and MβCD used were 10 μM, 100 μM, and 10 mM, respectively. Cells were preincubated with these compounds for 30 min.

caused cell killing mainly through their pore-forming activity, reports from recent years highlight that their manner of causing cell damage is complex, intriguing, and still not fully understood.

We show here that ACT induces an increase in cytosolic calcium that is independent of the presence of its integrin receptor CD11b/CD18, and compatible with extracellular calcium entering the cytosol following PKA activation, via toxin-produced cAMP, and activation of calcium channels with L-type properties that are not voltage gated. Confirmation of the presence of such functional L-type-like calcium channels in the J774A.1 macrophages used in this work has been presented. The temperature dependence of cation entry reflects the requirement for the translocation of the AC domain to ensure cAMP formation, a process that is very sensitive to temperature, and the high sensitivity to cholesterol depletion by MβCD suggests that it takes place in membrane microdomains, what might be explained by a localization of L-type-like calcium channels in such domains and by the finding that cAMP production by ACT is also significantly affected by this cholesterol sequestering agent. The toxin itself must probably insert into cholesterol-rich microdomains for translocation to happen. Finally, our findings demonstrate that ACT induces a calcium increase apparently through a common mechanism, *i.e.* the opening of cAMP-dependent L-type-like calcium channels, both in $CD11b/CD18^+$ and $CD11b/CD18^-$ cells.

In the work of Fiser *et al.* (14) translocation of the toxin AC domain was shown to be essential for the toxin to induce a sustained calcium elevation. The primary consequence of this domain translocation is the formation of high levels of cAMP, a second messenger broadly known to act through activation of protein kinase A. PKA, in turn, is known to phosphorylate, thus activate, L-type calcium channels. Their observation that exposure of the $CD11b^+$ cells to the cell-permeable cAMP analog db-cAMP (1 mM) had no effect on $[Ca^{2+}]_i$ led them to the conclusion that calcium entry was not mediated by cAMP. Using another cAMP-permeable analog, 8-Br-cAMP, we observed (data not shown) that this compound induced a very slow but measurable $[Ca^{2+}]_i$ rise. This much smaller effect of the cyclic nucleotide analog might be due to a low or slow permeability of the molecule across the cell plasma membrane or even to the fact that the molecule might enter along the whole membrane and not in a localized way, thus perhaps not reaching the necessary analog concentration to locally activate PKA. Our data support the observation by Fiser *et al.* (14) that the adenylate cyclase active center mutant K58Q does not allow Ca^{2+} entry, while adenylate cyclase domain translocation remains unaltered. In agreement with this idea, we found that forskolin, an activator of adenylate cyclases, many of which are concentrated in membrane domains (47), produced a rapid and very significant $[Ca^{2+}]_i$ rise that also decreased rapidly, probably due to the action of associated phosphodiesterases. This observation and our finding that the calcium influx induced by ACT might also take place in RLMD led us to underline the importance that a specific localization of calcium entry may have.

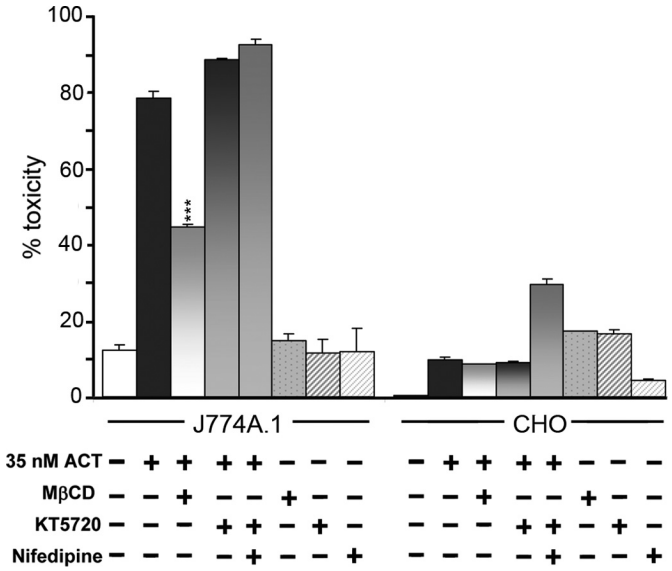

FIGURE 7. **Effect of calcium influx blocking and cholesterol depletion on the ACT-induced cytotoxicity.** Cell toxicity was determined by LDH assay as described under "Experimental Procedures." The concentrations of nifedipine, MβCD, and KT5720 used were 10 μM, 10 mM, and 56 μM, respectively. Cells were preincubated with these compounds for 30 min.

A localized $[Ca^{2+}]_i$ rise might be essential to activate certain signaling routes and not others, which in turn may influence the cellular effects triggered. The essential role played by a precise temporal and spatial organization of Ca^{2+} signaling has been addressed in several works. Petersen and Tepikin (48) described the influence of a precise spatial organization in the release of Ca^{2+} by the $InsP_3Rs$ in the apical region of pancreatic acinar cells that was confined by a mitochondrial firewall. At high agonist concentrations, this firewall was shown to be breached, and Ca^{2+} broke out and spread throughout the cell as a global signal. This local to global transition was proposed to alter the distribution of calmodulin (CaM), which concentrated in the apical region at low agonist doses but entered the nucleus when Ca^{2+} spread globally. Philipova *et al.* (49) described changes in the spatial organization of CaM that occurred during mitosis in sea urchin eggs. CaM localized around the nucleus at nuclear envelope breakdown (NEBD) and then concentrated at the two spindle poles later in mitosis. Beaumont *et al.* (50) described how the voltage-operated channels (VOCs) at the synaptic endings of bipolar ganglion neurons arranged in close proximity to the synaptic vesicles. They showed, using total internal reflection fluorescence microscopy (TIRFM) that Ca^{2+} entering through a VOC created a microdomain that activated vesicles within a radius of ~200 nm. Chasserot-Golaz *et al.* (51) described the geographical arrangement of the many signaling components responsible for triggering exocytosis in chromaffin cells. They identified a role for phospholipase D1 (PLD1) that might participate by bending the plasma membrane through phosphatidic acid, prior to exocytosis. The activation of PLD1 depended upon the small GTPase Arf6, located in the vesicle membrane, binding to ARNO attached to the plasma membrane. These signaling complexes appeared to be organized at the sites of exocytosis by lipid rafts that may be stabilized by annexin-2.

Intracellular calcium alterations are reported to be involved in processes leading to cell death such as apoptosis or necrosis (52, 53). ACT is able to induce both types of cell death (54); however, in this case the toxin-induced calcium rise is not directly involved in ACT-induced cytotoxicity, as shown here by the null effect of calcium entry blockers, La^{3+} or nifedipine. Studies in progress in our laboratory are aimed at elucidating the precise downstream effects of ACT-induced Ca^{2+} entry in cells.

Acknowledgments—We thank Prof. F. M. Goñi for critically reading the manuscript, Prof. A. Marino for assistance with $[Ca^{2+}]$ measurements, and Prof. J. López-Barneo and Dr. K. Levitsky for assistance in patch clamp experiments.

REFERENCES

1. Goodwin, M. S., and Weiss, A. A. (1990) *Infect. Immun.* **58,** 3445–3447
2. Glaser, P., Sakamoto, H., Bellalou, J., Ullmann, A., and Danchin, A. (1988) *EMBO J.* **7,** 3997–4004
3. Iwaki, M., Ullmann, A., and Sebo, P. (1995) *Mol. Microbiol.* **17,** 1015–1024
4. Welch, R. A. (2001) *Curr. Top. Microbiol. Immunol.* **257,** 85–111
5. Hewlett, E. L., Gray, L., Allietta, M., Ehrmann, I., Gordon, V. M., and Gray, M. C. (1991) *J. Biol. Chem.* **266,** 17503–17508
6. Rhodes, C. R., Gray, M. C., Watson, J. M., Muratore, T. L., Kim, S. B., Hewlett, E. L., and Grisham, C. M. (2001) *Arch. Biochem. Biophys.* **395,** 169–176
7. Confer, D. L., and Eaton, J. W. (1982) *Science* **217,** 948–950
8. Hanski, E., and Farfel, Z. (1985) *J. Biol. Chem.* **290,** 5526–5532
9. Bellalou, J., Sakamoto, H., Ladant, D., Geoffroy, C., and Ullmann, A. (1990) *Infect. Immun.* **58,** 3242–3247
10. Szabo, G., Gray, M. C., and Hewlett, E. L. (1994) *J. Biol. Chem.* **269,** 22496–22499
11. Benz, R., Maier, E., Ladant, D., Ullmann, A., and Sebo, P. (1994) *J. Biol. Chem.* **269,** 27231–27239
12. Hewlett, E. L., Donato, G. M., and Gray, M. C. (2006) *Mol. Microbiol.* **59,** 447–459
13. Basler, M., Masin, J., Osicka, R., and Sebo, P. (2006) *Infect. Immun.* **74,** 2207–2214
14. Fiser, R., Masín, J., Basler, M., Krusek, J., Spuláková, V., Konopásek, I., and Sebo, P. (2007) *J. Biol. Chem.* **282,** 2808–2820
15. Gerbig, D. G., Jr., Walker, R. D., Baker, J. C., Foster, J. S., and Moore, R. N. (1989) *Vet. Microbiol.* **19,** 325–335
16. Ortiz-Carranza, O., and Czuprynski, C. J. (1992) *J. Leukoc. Biol.* **52,** 558–564
17. Cudd, L., Clarke, C., Clinkenbeard, K., Shelton, M., Clinkenbeard, P., and Murphy, G. (1999) *FEMS Microbiol. Lett.* **172,** 123–129
18. Iwase, M., Korchak, H. M., Lally, E. T., Berthold, P., and Taichman, N. S. (1992) *J. Leukoc. Biol.* **52,** 224–227
19. Shenker, B. J., Vitale, L. A., Keiba, I., Harrison, G., Berthold, P., Golub, E., and Lally, E. T. (1994) *J. Leukoc. Biol.* **55,** 153–160
20. Hsuan, S. L., Kannan, M. S., Jeyaseelan, S., Prakash, Y. S., Sieck, G. C., and Maheswaran, S. K. (1998) *Infect. Immun.* **66,** 2836–2844
21. Fong, K. P., Pacheco, C. M., Otis, L. L., Baranwal, S., Kieba, I. R., Harrison, G., Hersh E. V., Boesze-Battaglia, K., and Lally, E. T. (2006) *Cell Microbiol.* **8,** 1753–1767
22. Uhlén P., Laestadius, A., Jahnukainen, T., Söderblom, T., Bäckhed, F., Celsi, G., Brismar, H., Normark, S., Aperia, A., and Richter-Dahlfors, A. (2000) *Nature* **405,** 694–697
23. Valeva, A., Walev, I., Kemmer, H., Weis, S., Siegel, I., Boukhallouk, F., Wassenaar, T. M., Chavakis, T., and Bhakdi, S. (2005) *J. Biol. Chem.* **280,** 36657–36663
24. Koschinski, A., Repp, H., Unver, B., Dreyer, F., Brockmeier, D., Valeva, A., Bhakdi, S., and Walev, I. (2006) *FASEB J.* . **20,** 973–975
25. Gao, Z., Young, R. A., Trucco, M. M., Greene, S. R., Hewlett, E. L.,

Matschinsky, F. M., and Wolf, B. A. (2002) *Biochem. J.* **368,** 397–404
26. Otero, A. S., Yi, X. B., Gray, M. C., Szabo, G., and Hewlett, E. L. (1995) *J. Biol. Chem.* **270,** 9695–9697
27. van der Goot, F. G., Tran van Nhieu, G., Allaoui, A., Sansonetti, P., and Lafont, F. (2004) *J. Biol. Chem.* **279,** 47792–47798
28. Llinás, R., Sugimori, M., and Silver, R. B. (1995) *Neuropharmacol.* **34,** 1443–1451
29. Yao, Y., Choi, J., and Parker, I. (1995) *J. Physiol.* **482,** 533–553
30. Berridge, M. J. (2004) *Biochim. Biophys. Acta* **1742,** 3–7
31. Isshiki, M., and Anderson, R. G. (2003) *Traffic* **4,** 717–723
32. Weerth, S. H., Holtzclaw, L. A., and Russell, J. T. (2007) *Cell Calcium* **41,** 155–167
33. Karimova, G., Fayolle, C., Gmira, S., Ullmann, A., Leclerc, C., and Ladant, D. (1998) *Proc. Natl. Acad. Sci. U.S.A.* **95,** 12532–12537
34. Grynkiewicz, G., Poenie, M., and Tsien, R. Y. (1985) *J. Biol. Chem.* **260,** 3440–3450
35. Okazaki, R., Iwasaki, Y. K., Miyauchi, Y., Hirayama, Y., Kobayashi, Y., Katoh, T., Mizuno, K., Sekiguchi, A., and Yamashita, T. (2009) *Int. Heart J.* **50,** 353–363
36. Stokes, L., Gordon, J., and Grafton, G. (2004) *J. Biol. Chem.* **279,** 19566–19573
37. Bergmeyer, H. U., and Bernt, E. (1974) in *Methods of Enzymatic Analysis* (Bergmeyer, H. U., ed), pp. 574–579, Vol. 2, Verlag Chemie Weinheim, Academic Press, New York and London
38. Guermonprez, P., Khelef, N., Blouin, E., Rieu, P., Ricciardi-Castagnoli, P., Guiso, N., Ladant, D., and Leclerc, C. (2001) *J. Exp. Med.* **193,** 1035–1044
39. Bassinet, L., Fitting, C., Housset, B., Cavaillon, J. M., and Guiso, N. (2004) *Infect. Immun.* **72,** 5530–5533
40. Paccani, S. R., Dal Molin, F., Benagiano, M., Ladant, D., D'Elios, M. M., Montecucco, C., and Baldari, C. T. (2008) *Infect. Immun.* **76,** 2822–2832
41. Colucci, A., Giunti, R., Senesi, S., Bygrave, F. L., Benedetti, A., and Gamberucci, A. (2009) *Arch. Biochem. Biophys.* **481,** 80–85
42. Grafton, G., Stokes, L., Toellner, K. M., and Gordon, J. A. (2003) *Biochem. Pharmacol.* **66,** 2001–2009
43. Das, R., Burke, T., Van Wagoner, D. R., and Plow, E. F. (2009) *Circ. Res.* **105,** 167–175
44. Maguy, A., Hebert, T. E., and Nattel, S. (2006) *Cardiovasc. Res.* **69,** 798–807
45. Gordon, V. M., Young, W. W., Jr., Lechler, S. M., Gray, M. C., Leppla, S. H., and Hewlett, E. L. (1989) *J. Biol. Chem.* **264,** 14792–14796
46. Harder, T., and Simons, K. (1997) *Curr. Opin. Cell Biol.* **9,** 534–542
47. Crossthwaite, A. J., Seebacher, T., Masada, N., Ciruela, A., Dufraux, K., Schultz, J. E., and Cooper, D. M. (2005) *J. Biol. Chem.* **280,** 6380–6391
48. Petersen, O. H., and Tepikin, A. V. (2008) *Annu. Rev. Physiol.* **70,** 273–299
49. Philipova, R., Larman, M. G., Leckie, C. P., Harrison, P. K., Groigno, L., and Whitaker, M. (2005) *J. Biol. Chem.* **280,** 24957–24967
50. Beaumont, V., Llobet, A., and Lagnado, L. (2005) *Proc. Natl. Acad. Sci. U.S.A.* **102,** 10700–10705
51. Chasserot-Golaz, S., Vitale, N., Umbrecht-Jenck, E., Knight, D., Gerke, V., and Bader, M. F. (2005) *Mol. Biol. Cell.* **16,** 1108–1119
52. Pinton, P., Giorgi, C., Siviero, R., Zecchini, E., and Rizzuto, R. (2008) *Oncogene* **27,** 6407–6418
53. Giorgi, C., Romagnoli, A., Pinton, P., and Rizzuto, R. (2008) *Curr. Mol. Med.* **8,** 119–130
54. Khelef, N., Zychlinsky, A., and Guiso, N. (1993) *Infect. Immun.* **61,** 14064–14071